Pre-print of the paper associated to doi.org/10.1016/j.microc.2023.108590

Spectroscopic and mass spectrometry-based *in-situ* investigation of a 17th-century handwritten academic diploma on illuminated parchment

Elena C. L. Rigante[a], Cosima D. Calvano*[a], Alessandro Monno[b], Martina Moroni[c], Gioacchino Tempesta*[b], Tommaso R.I. Cataldi[a]

[a] Dipartimento di Chimica, Università di Bari, via Orabona 4, 70125 Bari;

[b] Dipartimento Geomineralogico, Università di Bari, via Orabona 4, 70125 Bari;

[c] Archivio di Stato di Bari, Via Pietro Oreste 45, 70123 Bari, Italy.

Number of Tables: 2

Number of Figures: 9

Supporting Information: yes

Keywords: binder in artworks, pigments, parchment, MALDI, in-situ digestion, micro-Raman.

*Author for correspondence, email: cosimadamiana.calvano@uniba.it, gioacchino.tempesta@uniba.it

Abstract

In 2008, more than 300 ancient scrolls, some of which were preciously illuminated, were recovered in Chicago (USA) after being stolen and illegally exported. These scrolls consisted of private and public documents, including papal and royal, dating from the 14th to the 19th century. The scrolls were returned to Italy and 42 of them, known as the Chicago Parchments, are now preserved at the State Archives of Bari (Italy). Among them was an illuminated academic diploma from the 17th century, known as the *doctoratus privilegium*, which was of particular interest to restorers and conservation scientists. To identify the pigments, painting binders, and animal skin origin of the parchment, non-invasive analyses were carried out on several points using portable X-ray fluorescence (XRF), µRaman, and fibre optic reflectance spectroscopy (FORS). Gold and silver decorations were confirmed by XRF, highlighting the significance of the document. A quasi-non-invasive sampling approach was used to analyze the painting binders by applying a trypsin-chymotrypsin enriched hydrogel for *in-situ* digestion of the proteinaceous material. The extracted binders were successfully identified as bovine and rabbit glues by both matrix-assisted laser desorption/ionization with time-of-flight mass spectrometry (MALDI-ToF-MS) and reversed-phase liquid chromatography with electrospray ionization tandem mass spectrometry (RPLC-ESI-MS/MS). By using bottom-up proteomics, the sheep skin origin of thin parchment samples was established from very small fragments that were digested in solution with trypsin.

1. INTRODUCTION

In Europe, parchment was the primary writing medium until the 12th century. Even after paper became more widespread due to the invention of printing, parchment was still used for important documents and miniatures because of its durability and strength [1]. Parchment is made by treating animal skin, usually from lambs, calves, sheep, or goats, with calcium hydroxide and sometimes sodium sulfide, and then finishing it with alum, oil, or chalk to create a suitable surface for inks and pigments [1,2]. Today, many ancient parchment specimens are preserved and analyzed to uncover the pigments, binders, and adhesives used in refined decorations and miniatures. In religious artworks, "gilding" was often used to show the opulence and luxury of monarchs, but many original gilded layers have been lost or replaced by restoration with cheaper interventions [3]. In this study, a parchment dating back to the XVII century (Figure 1) was investigated using a multi-technique approach to uncover the chemical composition of its refined decorations in terms of pigments, painting binders, and animal skin origin. The parchment that was studied is part of a collection of ancient manuscripts, documents, coins, and other archaeological items that were illegally exported from Italy, particularly Apulia, to Illinois, USA, between 1964 and 2000 as part of an illicit trade. In 2007, the valuable items were discovered and returned to their rightful owners, which included diocesan museums, libraries, and archives, in a joint effort by the Chicago Federal Bureau of Investigation (FBI) and the Italian Carabinieri Unit for Cultural Heritage Protection. Along with more than 40 scrolls, which are now known as the Chicago Parchments, the parchment studied in this work has been kept at the State Archives of Bari (Italy) since 2017 since its origin could not be determined. It represents a *doctoratus privilegium*, namely a diploma degree in canonical and civil law, conferred in 1663 to Vito Lorenzo Gonnella of Turi (Bari, Italy) by Francesco Marino Caracciolo Arcella, royal chancellor and prince of Avellino (Naples, Italy). The

artefact was in a fair state of conservation, due to the dehydration and parchment distortions with consequent cracks and discolour spread all over the painting surface, mainly on the golden areas. Moreover, several losses were on the bottom edge, one on the right side and some in Gonnella's stemma. A diagnostic campaign was mandatory to discover the object's manufacture and artistic techniques and also adequately safeguard its restoration, which often represents a challenging task due to degradation phenomena such as morphological damages [4], gelatinization [5], and fungal and microbial attacks [6,7].

To identify the inorganic pigments in ancient illuminated manuscripts, non-destructive and non-invasive techniques such as portable micro-Raman and micro-XRF are the most suitable and widely used methods [8–13]. *In situ* vibrational spectroscopic analyses, including external reflection-FTIR, attenuated total reflection (ATR) – FTIR [14], and near-infrared imaging, have been proposed to distinguish between protein- and lipid-based binders, exploiting characteristic methylene and amide vibrational modes [15,16]. To recognize the animal origin of ancient parchments, including whether goat, sheep, or bovine skin was used, recent advances in the omics field such as DNA analysis (genomics) and proteomics have been obtained by mass spectrometry [17,18]. Several authors have successfully used a non-destructive and non-invasive multi-approach for pigment identification in parchments, using complementary analytical techniques [19–28]. Historical pigment reference databases [29–31] are a valuable resource for identifying pigments through XRF, FORS, and Raman.

In this study, the use of portable instruments like XRF, FORS, and micro-Raman spectroscopy made it possible to identify inorganic pigments in a non-invasive way. Likewise, the presence of gold and silver was examined as part of the bright ornamentation in the text. To identify the painting binders, a proteomic strategy was employed, utilizing mass spectrometry (MS)-based techniques such as liquid chromatography with electrospray ionization (LC-ESI-MS) and matrix-

assisted laser desorption/ionization with time-of-flight (MALDI-ToF-MS) [32][33,34]. By analyzing proteinaceous binders and adhesives based on caseins, egg, and animal glues, this approach was able to identify various ancient art pieces, including frescoes [35] or wooden, sandstone, and precious alabaster polychromies [36]. Furthermore, species-specific peptides were defined to assess the origin of ancient parchment folios [37,38]. FTIR and Raman spectroscopies were used to distinguish between different binder types (proteins, lipids, polysaccharides) and identify single chemical compounds [10,39]. However, MS-proteomics allows for more accurate recognition of proteins contained in the sample and their relative coverage percentage.

A quasi-non-invasive protocol for in-situ protein digestion was employed, which overcame the drawback of material removal with micro-sampling. This approach was recently tested on various historical samples, such as paintings and stony or wooden sculptures [40–42]. The combined *in-situ* and in-solution digestion made it possible to identify bovine and rabbit glue as painting binders, alongside some mouse collagen residues and sheep skin as parchment material. This approach was successfully applied to identify the palette and binding media used to illuminate this precious XVII-century parchment.

2. MATERIALS AND METHODS

2.1. Chemicals. Water LC-MS grade, acetonitrile (ACN) LC-MS grade, formic acid (FA), ammonium bicarbonate, α-cyano-4-chloro-cinnamic acid (CClCA), dithiothreitol (DTT), iodoacetamide, trypsin (Proteomics Grade from the porcine pancreas) and chymotrypsin (Sequencing Grade from bovine pancreas) were obtained from SigmaAldrich (Milan, Italy). RapiGest SF Surfactant was purchased from Waters. ZipTip® pipette tips with 6 µL C18 resin were acquired from Millipore. Nanorestore Gel® Medium Water Retention - ("Extra Dry", Italian

Patent from Consorzio CSGI, University of Florence) is a poly(2-hydroxyethyl methacrylate)/poly(vinylpyrrolidone) (PHEMA/PVP) hydrogel [43–46].

2.2. Samples. For pigments analysis, 39 sample points were investigated as specified in figure 1 with codes starting with P. Letter G in figure 1 indicates seven points where the hydrogel protocol for binders extraction was applied. To analyze small parchment remains, weighing between 0.6-0.8 mg and labelled as S1, S2, and S3 in Figure 1, enzymatic digestion was performed.

2.3. Non-invasive in situ analysis. An accurate and preliminary selection of the parchment was carried out by an optical microscope to choose the surface sampling points. Most selected areas were examined by FORS; this technique has the advantage of being quick for pigment identification and it is based on standard spectra comparison [30]. To confirm the initial information obtained by FORS and to obtain a chemical fingerprint, XRF analyses were performed by a sampling of at least four points for each colour. In some doubtful cases, μ-Raman spectra were collected. The spectra referred to not miniated areas were used as substrate backgrounds.

2.4. Micro-Raman. Due to the difficulties connected to the shape and the dimensions of the parchment in using the Raman mobile instrumentation, these analyses were performed in just six points, where FORS and XRF data were not univocally explainable. A micro-Raman system by Horiba Jobin Yvon (France SAS), equipped with a red He-Ne laser (632.8 nm) and optical fibres, was used. Low laser power on the sample, 1 mW, guaranteed parchment safety, while the frequency calibration was performed against a silicon Raman peak (520 cm^{-1}). The instrument, equipped with an optic head with a 50X objective, exhibits a spot size of 1 μm across and a spectral resolution of 10 cm^{-1}. Acquisitions were performed with LabSpec 4.18 software while the data elaboration (baseline correction, normalization, smoothing) and the

identification of the analysed phases were performed with Spectragryph [47] using the minerals reference spectra acquired from the RRUFF database [48].

2.5. FORS. FORS analysis was carried out with a custom system by Avantes (B.V. Netherlands). The AvaSpec-ULS2048XL- USB2 model spectrophotometer and an AvaLight-HAL-S tungsten halogen light source were combined with a reflection probe FCR-7UV200-2-ME UV/VIS. The spectra were recorded with a 1.4 nm spectral resolution in the range of 350 to 1000 nm to avoid noise in UV and IR regions. The possibility to collect a reflectance spectrum from a small area, guaranteed by the diameter of the probe (ca. 200 µm), was crucial to avoid inhomogeneous coloured areas, especially when the surface was damaged or fractured with the tampering of time. Diffuse reflectance spectra of the samples were compared against the WS-2 reference tile, assured to be reflective at 98% or more in the spectral range investigated. The FORS spectra of 35 painted areas, with spot sizes about 2 mm in diameter, were acquired on the parchment. In all measurements, the distance between the probe and sample was fixed, i.e. ca. 5 mm. The instrumental parameters were as follows: 10 ms integration time and 100 scans for a total acquisition time of 1 s for each spectrum. The spectra were collected with Avasoft 8.0 and then exported in Spectragryph [47] for processing, mathematical operations, and standard comparison.

2.6. XRF. Twenty points were analysed *in situ* with a custom portable XRF instrument. The X-ray source is an AMPTEK (Inc. USA) Mini-X with Au target, operating at 40 kV and 95 µA. The detector is a silicon drift (SDD) Amptek XR-123 SDD with a 25 mm^2 detection area, 500 µm thickness (fully depleted) and a 12.5 µm Be window. Resolution at 5.9 keV is 135 eV at room temperature. The system is equipped with two laser pointers to identify the central point of the X-ray beam at a 90° angle from the detector axis. This geometry allows partially polarized radiation with a high background reduction on Compton scattering. Samples were analysed

directly on air at room temperature. The outgoing radiation is collimated in a 5 mm beam diameter at the sample surface. Each acquisition had a fixed working distance (15 mm) between the instrument and the parchment surface controlled by a laser interferometer. The acquisition time for each spectrum was 60 s. The spectra for qualitative analyses were collected and elaborated with the software Surface Monitor 7.0. XRF analysis performed in the air generates some physical limits in lighter elements detection. In our case, with the previously described setup, only elements with Z equal to or higher than 16 (S) were detectable.

2.7. ATR-FTIR. ATR-FTIR analyses were carried out using a Spectrum Two Perkin Elmer (Milan, Italy) instrument equipped with a diamond prism. Spectra acquired in reflectance mode were converted in transmittance mode within the range 400-4000 cm^{-1} accumulating 32 scans per spectrum with a resolution of 4 cm^{-1}. Air spectra were registered as background. Raw ATR-FTIR spectra were acquired and processed with Spectrum 10™ software (Perkin Elmer, Milan, Italy), exported in txt format, and plotted using OriginPro 2015.

2.8. Dual-enzyme *in-situ* digestion. Small pieces (3 mm × 3 mm) of PHEMA/PVP hydrogel [46] were dried until they lost 20% of their weight and loaded with 20 µL of trypsin and 20 µL of chymotrypsin aqueous solutions (both 20 µg/mL) for 30 min. Each piece of hydrogel-containing enzymes was applied upon the parchment surface for 30 min for *in-situ* digestion of protein-based binders. The hydrogel was immersed into 100 µL of a 70:30 ACN:H_2O with 0.1% FA solution and left for 20 min in an ultrasonic bath at 30 °C to promote the release of peptides. Such a solution was vacuum-dried, reconstituted in 20 µL of 95:5 ACN:H_2O 0.1% FA and analysed by MALDI-ToF-MS and/or RPLC-ESI-MS(/MS) [40,41]. In cases of high background spectra, the sample mixture was vacuum dried, redissolved into 50 µL FA 0.1%, purified using a C18 ZipTip and eluted with 10 µL 95:5 ACN:H_2O FA 0.1%.

2.9. Tryptic in-solution digestion. Three fragments of the parchment (samples S1, S2 and

S3), weighing between 0.6-0.8 mg, were enzymatically digested in solution. They were added with 80 µL of RapiGest reagent (Waters Corporation, Milan, Italy) (1 mg/mL in NH_4HCO_3 50 mM) and kept at 60 °C for 1 hour. 10 µL of 50 mM DTT were added and the mixture was incubated at 60 °C for 20 min to reduce disulphide bonds between cysteines. Thiols alkylation was performed with 10 µL of 150 mM iodoacetamide and the solution was kept in the dark at room temperature for 15 min. Finally, the mixture was added with 8 µL of sequencing-grade trypsin solution (20 µg/mL) and incubated at 37 °C overnight. Enzymatic digestion was stopped by adding 5 µL of formic acid 98%. A C18 ZipTip® purification protocol was also performed to remove inorganic salts and preconcentrate the sample before MS analysis.

2.10. MALDI-ToF-MS. A 5800 MALDI-ToF/ToF analyzer (AB SCIEX, Darmstadt, Germany) equipped with a neodymium-doped yttrium lithium fluoride (Nd:YLF) laser (345 nm) was employed in reflectron positive mode, with 10 ppm mass accuracy. Analysis was performed on both in-solution and in-situ digested samples. 3 µL of the analyte solution were mixed 1:1 (v:v) with MALDI matrix CClCA (10 mg/mL in 70:30 ACN:H_2O and 0.1% TFA). 1 µL of the mixture was deposited on the target plate, dried at room temperature, and washed on spot with 1 µL H_2O LC-MS grade. External calibration was accomplished using a mixture containing renin, angiotensin I and ACTH in the range of 800-4000 *m/z*. 1000 laser shots were acquired at laser pulse rates of 400 Hz and each mass spectrum resulted from an average of six spectra at least. The delayed extraction time was set at 240 ns. The software Data-Explorer 4.11 was used for visualization of raw MALDI-MS data and conversion in txt files; mMass 5.5.0.0. was employed for mass spectra elaboration and peak lists extraction.

2.11. RPLC-ESI-MS/MS. Liquid chromatographic analyses with tandem MS experiments were performed using an Ultimate 3000 UHPLC coupled to HESI (heated electrospray ionization) interface and VelosPro mass spectrometer (Thermo Scientific, Waltham, MA, USA) equipped

with a double linear trap mass analyzer. Column Ascentis® Express C18 (15 cm x 2.1 mm ID, 2.7 µm particles) with guard column Ascentis® Express C18 (5 mm x 2.1 mm ID) (Supelco, Sigma-Aldrich Chemie GmbH, Germany) was set at 40 °C during runs. Chromatographic separation was performed at 0.2 mL/min flow with mobile phases H_2O with 0.1% FA in volume (phase A) and ACN with 0.1% FA in volume (phase B). The chromatographic gradient was set as follows: min 0-2 5% B phase isocratic; min 2-12 from 5% to 35% B phase, min 12-17 35% B phase isocratic, min 17-35 from 35% to 100% B phase, min 35-37 100% B phase, min 37-39 from 100% to 5% B phase, min 39-44 5% B phase isocratic. For MS acquisitions, parameters were set as follows: sheath gas flow rate 30 a.u. (arbitrary units); auxiliary gas flow rate 15 a.u.; spray voltage 2.5 kV; capillary temperature 275 °C; S-Lens radio frequency level 60 a.u. Acquisitions were performed in positive ion mode within the *m/z* interval 130-2000 and collisionally induced ionization (CID) energy was set as 35% u.a. for MS/MS ions fragmentation. The software Xcalibur 2.2 SP1.48 (Thermo Scientific) was used for raw RPLC-MS data while mMass 5.5.0.0. was employed for spectra elaboration and peak lists extraction.

2.12. Bioinformatic research. MALDI-ToF-MS PMF obtained from both in-situ and in-solution digestion protocols were interpreted using the online software Protein Prospector MS Fit (University of California, San Francisco https://prospector.ucsf.edu/prospector/cgi-bin/msform.cgi?form=msfitstandard) for proteins identification. Peptides sequences were identified by RPLC-ESI tandem MS data using Protein Prospector MS Tag (https://prospector.ucsf.edu/prospector/cgi-bin/msform.cgi?form=mstagstandard). In both cases, the search was performed with the databases SwissProt.2021.06.18 and UniProtKB2020.09.02 among all taxonomies, with tolerance set on 0.2 Da and four acceptable missed cleavages. Peptide variable modifications were chosen as follows: oxidation of methionine, proline and tryptophan, deamidation of asparagine and glutamine and

238 phosphorylation of serine, threonine and tyrosine. In the case of in-solution digested samples,
239 also carbamidomethylation of cysteine was set as a constant modification. Some searches were
240 run with the option "no enzyme" to allow MS/MS spectra interpretation of non-specific
241 peptides.
242
243 **3. RESULTS AND DISCUSSION**
244 **3.1. Spectroscopic analysis**
245 The portable XRF instrument allowed the parchment examination with the detection of calcium
246 and very negligible traces of sulfur and chlorine (Fig. 2); these elements are most likely due to
247 remnants of materials used for parchment-making processes [49]. The appearance of signals
248 from Fe, Ni, Cu, and Zn in the spectrum may be attributed to the instrument components,
249 specifically the slit and case. To achieve white surfaces and reduce hide moisture content,
250 materials such as NaCl, lime (CaO), pumice stone (SiO_2+Al_2O_3) [9] and chalk ($CaCO_3$) were
251 commonly used. However, these materials also generate XRF spectra with a complex chemical
252 background, and the binding medium produces strong fluorescence that interferes with the
253 acquisition of useful Raman spectra for blue and green sampled elements.
254 **3.1.1 Red pigments**
255 The spectroscopic analyses performed on 8 points of the red areas on the parchment allowed
256 us to identify the pigments. In areas where the red colour was intense, both XRF data and
257 Raman spectra identified two pigments. However, in areas with a lighter shade of red, only one
258 pigment was recognized. The pigments identified were vermillion, corresponding to cinnabar
259 (HgS), and red lead, corresponding to minium (Pb_2PbO_4). The FORS spectra confirmed the
260 presence of both minium and cinnabar pigments. The inflection points at 560-590 nm were
261 shifted by 30 nm, suggesting a mixture of minium and cinnabar. This was confirmed by PXRF

analysis, which detected both Pb and Hg. The Raman spectra and PXRF data provide conclusive identification of the chemical composition of pigments. By comparing the spectra with the RRUFF minerals database [48] (Fig. 3), we verified the presence of the main vibrational bands of minium (543, 389 cm^{-1}) and cinnabar (342, 288, 253 cm^{-1}). By detecting the presence of Pb, minium was identified in the PXRF analysis, while the presence of Hg allowed us to identify cinnabar (Fig. S2).

3.1.2 Blue pigments

Nine points on the parchment were found to contain azurite (i.e. 2CuCO3·Cu(OH)2) and smalt (potassium glass containing cobalt). Azurite was detected in the external part of the parchment, where blue decorations were present, by FORS and PXRF analyses. However, the Raman spectrum of azurite could not be conclusively identified due to the strong fluorescence signal from the binder. On the other hand, a Raman spectrum of smalt was obtained from the blue area surrounding the text. The main peak was at 463 cm^{-1} in good agreement with the Raman spectrum database of smalt [29] (Fig. S3). FORS and PXRF analyses confirmed the presence of smalt. The red-IR region of the FORS spectra allowed us to distinguish between azurite and smalt. Some points, such as Pb8, contained smalt, while others, like Pb5, had a mixture of smalt and azurite (Fig. S4). The identification of Co for smalt and Cu for azurite in the PXRF spectra also confirmed the presence of both pigments (Fig. S5).

3.1.3 Green pigment

Malachite, a copper carbonate hydroxide mineral ($CuCO_3$ $Cu(OH)_2$), is the most likely green pigment given the age of the parchment. However, we could not record a Raman spectrum of malachite due to the strong fluorescence caused by the binder. FORS spectra resemble malachite (Fig. S6), while PXRF analyses show the presence of Cu, Pb, and As (Fig. S7). While Pb is due to white lead, the presence of As could be attributed to Emerald green (Schweinfurt

green) or Scheele's green. Further examination using other methods is required to distinguish between these pigments. As with the blue and red pigments, this could confirm later retouching of the parchment.

3.1.4 Metal coatings

The parchment features a design of a double-headed eagle with spread wings, adorned with gold feathers, all enclosed in a frame of floral patterns. The text of the *privilegium* is situated within an oculus, surrounded by a blue frame and intricate silver friezes. Analysis using XRF confirmed the use of precious metals in the gold and silver decorations (Fig. 4). Interestingly, some of the feathers without gold decoration showed the use of adhesive layers made with a mixture of soft iron-containing clay (bole) and glue [50]. This reveals how the thin layers of pure gold were applied to the parchment. The presence of glue, as mentioned in the literature [50], is further supported by proteomic analysis.

3.2 Analysis of binders and/or parchment by ATR-FTIR spectroscopy

Non-destructive ATR-FTIR analyses were performed on fragments S2 and S3 of the parchment, which did not contain any decorations. In Figure 5, the acquired spectra on both sides of sample S2 are shown to characterize the scroll. For simplicity, the two sides are labelled as A and B because distinguishing between the grain and hair side was a difficult task. No significant spectral differences were detected except for a low-intensity band at 1279 cm^{-1} on the B side due to C-O stretching [51]. The spectra show typical IR bands of collagen, such as amides *I* and *II* at 1630 and 1540 cm^{-1}, a weaker band of amide *III* at 1235 cm^{-1}, amide A and amide B at 3290 and 3079 cm^{-1}, respectively [51,52]. The strong and broad transmittance band at 1410 cm^{-1} is the result of at least three contributions, namely C-O-H and NH2 bending, both at about 1450 cm^{-1} [51,53] and carbonate v3 asymmetric stretching at 1390-1410 cm^{-1} attributable to $CaCO_3$. The sharp signals at 873 and 712 cm^{-1} refer to v2 asymmetric and v4 symmetric CO_3^{2-} stretching

while v1 vibrational mode generates a weak signal at 1079 cm^{-1} [54–56]. The presence of calcium carbonate was already reported in ancient parchments by Mannucci [52] and Bicchieri [21]. Ancient pre-treatments carried out in western Europe involved immersing animal skin into a Ca(OH)2 solution [1,21,57] which resulted in the formation of $CaCO_3$ after the air reaction. A couple of weak bands at 1080 and 1031 cm-1 were assigned to proline ring stretching vibrations [58]. Recent studies [59–62] have shown that collagen triple helix denaturation into random coil structures due to parchment aging produces a shift of the amide *II* band towards lower wavenumbers so that the delta (Δ) between amide *I* – amide *II* enlarges. As demonstrated by Cappa *et al*. [61,62], gelatinization is very advanced when Δ is higher than 100, which was not the case in our samples. However, CH_2 asymmetric and symmetric stretching at 2851 and 2920 cm^{-1} were much more intense than asymmetric and symmetric CH_3 stretching at about 2890 and 2950 cm^{-1}, suggesting that collagen denaturation is occurring to some extent, thus facilitating backbone vibration [63]. To distinguish between binder and parchment material, a proteomic approach was used.

3.3 MS-based analysis of binders by *in situ* digestion

To analyze specific sample zones labelled as Gbolo2, Gb5, Gg4, Gb11, Gdec and Gr6 in Figure 1, a hydrogel protocol was used. Because the composition of the binders was unknown, in situ digestion with two enzymes was performed, which is known to be effective for egg- and casein-based binders with high protein coverages [41]. Figure 6 shows the MALDI-MS spectrum of sample Gb11, which corresponds to a point on the left of the blue-painted frame where the text is included. The spectrum was reported from *m/z* 850.0 to exclude the high-intensity signal of trypsin at m/z 842.5, which was useful for internal mass calibration. Although the S/N ratio is relatively low due to the small amount of extracted sample and the presence of protective coatings on historically aged artworks, such as varnish and polysaccharides [38,64], a typical

tryptic/chymotryptic digestion pattern of animal collagen chains was recognizable. This suggests the use of animal glue, with marker peaks at *m/z* 1105.6, 1267.7, 1427.7, 1459.7, 1975.9, and 2131.0, consistent with previous research [65–70]. Most of the peptides were interpreted as belonging to bovine collagen chains (taxonomy *Bos taurus*) such as alpha-1(I), alpha-1(II), alpha-2(1) using Protein Prospector to confirm the data. However, additional evaluations were required to determine whether glues from other animal species were also employed [40,42,69]. This is because high similarities exist between protein sequences of mammals, and the SwissProt and NCBInr databases are incomplete regarding collagen chain sequencing of mammals other than bovine. Nevertheless, peptides at *m/z* 972.5, 1110.5, 1221.6, 1921.9, and 2092.9 were successfully assigned to rabbits (*Oryctolagus cuniculus*) as reported by Romero-Pastor et al. [71] and Buckley et al. [72] by MALDI-MS/MS.

For unambiguous identification, peptides generated from a mixture of proteins in a complex sample, where several isobaric and isomeric peptides are presumably present, the digested samples were chromatographically separated and each isolated peak signal fragmented in CID mode using a linear trap analyzer. Figure 7 presents RPLC-ESI(+)-MS/MS spectra of three ions obtained after hydrogel in situ digestion. Figure 7A shows the fragmentation pattern of the double-protonated ion at m/z 860.4, corresponding to the monocharged m/z 1719.8. The main peaks of the spectra were assigned to *y* and *b*-type ions generated from the cleavage of peptide bonds, allowing for recognition of the sequence (R)GARGEP(Ox)GPAGLP(Ox)GPP(Ox)GER(G)2+ generated from the tryptic proteolytic activity at the arginine carboxyl side of the collagen alpha-1(I) chain of *B. taurus*. Notably, proline oxidation in hydroxyproline is a common post-translational modification in collagen chains.

The glycine-proline-hydroxyproline triplets are commonly found in these proteins [73] and are usually considered markers of mammal collagen in Py-GC/MS [18,33]. However, the exact

sequence position of hydroxyprolines is hard to establish since at least nine possible combinations exist, and other minor sequences cannot be ruled out. The sequence herein proposed, with the first, third and fifth proline oxidized, had the highest score in bioinformatic research as it can better explain the MS/MS spectrum. Spectrum in panel B was assigned to (P)QGIP(ox)GTPGRPG(V)2+ of bovine collagen alpha-1(XVII) chain having m/z 526.8 as double-charged and m/z 1052.5 as mono-protonated, which is the base peak in the MALDI-MS spectrum of Figure 6. Similarly, ion at m/z 972.4 (Figure 7C) is imputable to an *aspecific* peptide coming from collagen alpha-1(XV) chain of rabbit, namely the sequence (D)AN(deam)DN(deam)FFVSG(P)+. Such sequences may be generated by hydrolysis processes during ageing degradation [2,74]. Some peptides were identified as mouse collagen chains, namely monocharged ions at m/z 1443.7, 1693.8, 2028.0 and 2265.0 corresponding to the GAAGPP(ox)GATGFP(ox)GAAGR (alpha-1(I)), GP(ox)IGQP(ox)GPSGADGEP(ox)GPR (alpha-1(V)), TGVP(ox)SFTKPVPPTQKP(ox)APF (alpha-I(XXVII)) and GYPGSIGPTGAAGAP(ox)GP(ox) HGSVGP(ox)AGK (alpha-2(I)).

The hydrogel sample likely extracted hair, saliva, and teeth residues left on the surface of the parchment due to rat activity over almost 40 years of storage. A list of assigned peptides and relative proteins is reported in Table 1 for the samples investigated with the hydrogel non-invasive protocol. Experimental findings allowed the identification of both bovine and rabbit collagen peptides, suggesting the use of a mixture of animal glues as painting binders. When only one or two peptides per protein were detected by MALDI-MS, Protein Prospector failed the identification, but structural assessment via RPLC-ESI-MS/MS analysis was successful.

In Figure 8, the tandem MS fragmentation of a double-charged ion at m/z 722.3 is shown, which we believe is due to rat activity over almost 40 years of storage. We suspected that hair, saliva, and teeth residues left on the surface of the parchment were extracted by the hydrogel sample.

A list of assigned peptides and relative proteins can be found in Table 1 for the samples investigated with the hydrogel non-invasive protocol. Our experimental findings allowed us to identify both bovine and rabbit collagen peptides, suggesting the use of a mixture of animal glues as painting binders. Protein Prospector failed to identify some proteins where only one or two peptides per protein were detected by MALDI-MS. However, we were able to accomplish a structural assessment via RPLC-ESI-MS/MS analysis.

To efficiently identify the parchment bulk material, a micro-sampling was needed because the enzyme proteolytic activity of the hydrogel in situ digestion protocol targets the most superficial layers of the parchment, which are likely to contain adhesives and binders. In addition, the digestion was carried out without denaturation and alkylating agents, which limits the number of cleavage sites available for the enzymes to target. Therefore, more effective solution digestion was performed on the micro-samples.

3.4 MS-based analysis of parchment by in-solution digestion

To discover the animal skin used, three small parchment fragments were conventionally digested “in solution” with trypsin. The results of the sample labelled as S1 are shown in Figure 9A. Although animal collagen was detected [65–70], the exact mammal species could not be unambiguously identified by the software, which is a common issue among scientists studying collagen. Efforts have been made to find species-specific peptides in PMF and tandem MS data. Buckley et al. [72] identified marker peptides of 32 different mammal species using MS coupled to multivariate analysis. The ion at m/z 2883.3 was shown to be a useful marker for distinguishing between sheep/goat and cow [37,72,76]; collagen alpha-1(I) contains the sequence GLTGPIGPPGPAGAPGDKGE**T**GPSGPAGPTGAR + two oxidations in sheep/goat and GLTGPIGPPGPAGAPGDKGEAGPSGPAGPTGAR + two oxidations in the cow peptide. Since the sequences differ in just one amino acid, they produce different peaks in the PMF at *m/z* 2883.4

for sheep/got and 2853.4 for the cow. The peak at *m/z* 2883.4 was revealed in the analysed samples as shown for sample S1 in Figure 9A. For structural confirmation, Figure 9B illustrates the fragmentation of the triple-charged ion at *m/z* 961.3, corresponding to monoprotonated ion at *m/z* 2883.4.

The analysis of the protein sequence using Protein Prospector software confirmed that the identified sequence belongs to either sheep or goat collagen (see Table S1). A list of sheep collagen peptide markers was also proposed [72] and fully retrieved in our PMF from samples S1, S2 and S3, namely peaks at *m/z* 1180.6, 1196.6, 1427.7, 1580.8, 2131.0, 2263.1, 2883.4 and 3017.4 (Figure 6A). However, oxidized forms of some peaks at *m/z* 2883.4 and 3017.4 (Δ=16 u), were not found. Peaks at m/z 1180.6, 1196.6, and 1580.8 were considered markers for ovicaprids, while the distinction between sheep and goat was based on the presence of specific ions at m/z 3017.4 in sheep and m/z 3077.4 in goat both belonging to collagen alpha-1(II) chain [37,72]. These outcomes suggest that the parchment material originated from sheep skin. A summary of the results from all investigated sample points can be found in Table 2.

4 CONCLUSIONS

This study focused on an illuminated parchment from the 17th century. By combining various spectroscopic and mass-spectrometric techniques, both the inorganic and organic materials used were identified. Specifically, FORS, XRF, and micro-Raman techniques were used to distinguish inorganic pigments like minium, malachite, and smalt, as well as silver and gold decorations. Meanwhile, MALDI-MS and RPLC-ESI-MS/MS were used to identify the sheepskin origin of the parchment material, as well as the use of a mixture of bovine and rabbit glue as a binder. Additionally, some traces of mouse collagen proteins were found, indicating damage from rats during almost 40 years of improper storage. By identifying both the pigments and

paint binders used in the parchment, it is more reasonable to choose the best approaches for cleaning the object, preserving its originality and protecting its painted surface.

ACKNOWLEDGMENTS

This work was supported by the project PONa3_00395/1 "BIOSCIENZE & SALUTE (B&H)" financed by the Ministero per l'Istruzione, l'Università e la Ricerca (MIUR). Authors wish to thank Vito Nettis for his help in running some proteomic experiments.

Author Contributions

C. D. Calvano, A. Monno, G. Tempesta: Conceptualization; E. C. L. Rigante, C. D. Calvano, A. Monno, G. Tempesta: Data curation; E. C. L. Rigante, C. D. Calvano, A. Monno, G. Tempesta: Formal analysis; T. R. I. Cataldi: Funding acquisition; E. C. L. Rigante, C. D. Calvano, A. Monno, G. Tempesta: Investigation; C. D. Calvano, A. Monno, G. Tempesta: Methodology; C. D. Calvano, A. Monno, M. Moroni, G. Tempesta: Supervision; C. D. Calvano, T. R. I. Cataldi, A. Monno, M. Moroni, G. Tempesta: Validation; E. C. L. Rigante, G. Tempesta: Writing - original draft; C. D. Calvano, T. R. I. Cataldi, A. Monno, M. Moroni: Writing - review & editing.

Conflict-of-interest

The authors declare no conflict-of-interest.

References

[1] M.L. Ryder, Parchment—Its History, Manufacture and Composition, J. Soc. Arch. 2 (1960) 391–399. doi:10.1080/00379816009513778.

[2] M. Bicchieri, M. Monti, G. Piantanida, A. Sodo, M. Tanasi, Inside the Parchment, in: 9th Int. Conf. NDT Art, 2008.

[3] I.C.A. Sandu, L.U. Afonso, E. Murta, M.H. De Sa, Gilding techniques in religious art

between east and west, 14th-18th centuries, Int. J. Conserv. Sci. 1 (2010) 47–62.

[4] K.M. Axelsson, R. Larsen, D.V.P. Sommer, R. Melin, Degradation of collagen in parchment under the influence of heat-induced oxidation: Preliminary study of changes at macroscopic, microscopic, and molecular levels, Stud. Conserv. 61 (2016) 46–57. doi:10.1179/2047058414Y.0000000140.

[5] L. Gonzalez, T. Wess, Use of attenuated total reflection-fourier transform infrared spectroscopy to measure collagen degradation in historical parchments, Appl. Spectrosc. 62 (2008) 1108–1114. doi:10.1366/000370208786049196.

[6] S. Fiddyment, M.D. Teasdale, J. Vnouček, É. Lévêque, A. Binois, M.J. Collins, So you want to do biocodicology? A field guide to the biological analysis of parchment, Herit. Sci. 7 (2019) 1–10. doi:10.1186/s40494-019-0278-6.

[7] E. joseph, ed., Microorganisms in the Deterioration and Preservation of Cultural Heritage, 2021.

[8] S. Bruni, F. Cariati, F. Casadio, L. Toniolo, Identification of pigments on a XV century illuminated parchment by Raman and FTIR microspectroscopies, Spectrochim. Acta - Part A Mol. Biomol. Spectrosc. 55 (1999) 1371–1377. doi:10.1016/S1386-1425(98)00300-X.

[9] M. Manso, A. Le Gac, S. Longelin, S. Pessanha, J.C. Frade, M. Guerra, A.J. Candeias, M.L. Carvalho, Spectroscopic characterization of a masterpiece: The Manueline foral charter of Sintra, Spectrochim. Acta - Part A Mol. Biomol. Spectrosc. 105 (2013) 288–296. doi:10.1016/j.saa.2012.11.110.

[10] S. Bruni, F. Cariati, F. Casadio, V. Guglielmi, Micro-Raman identification of the palette of a precious XVI century illuminated Persian codex, J. Cult. Herit. 2 (2001) 291–296. doi:10.1016/S1296-2074(01)01131-1.

[11] T. Lachmann, G. Van Der Snickt, M. Haschke, I. Mantouvalou, Combined 1D, 2D and 3D micro-XRF techniques for the analysis of illuminated manuscripts, J. Anal. At. Spectrom. 31 (2016) 1989–1997. doi:10.1039/c6ja00220j.

[12] G. Van Der Snickt, W. De Nolf, B. Vekemans, K. Janssens, µ-XRF/µ-RS vs. SR µ-XRD for pigment identification in illuminated manuscripts, Appl. Phys. A Mater. Sci. Process. 92 (2008) 59–68. doi:10.1007/s00339-008-4447-9.

[13] E. Calà, A. Agostino, G. Fenoglio, V. Capra, F. Porticelli, F. Manzari, S. Fiddyment, M. Aceto, The Messale Rosselli: Scientific investigation on an outstanding 14th century

illuminated manuscript from Avignon, J. Archaeol. Sci. Reports. 23 (2019) 721–730. doi:10.1016/j.jasrep.2018.12.001.

[14] L. Nodari, P. Ricciardi, Non-invasive identification of paint binders in illuminated manuscripts by ER-FTIR spectroscopy: a systematic study of the influence of different pigments on the binders' characteristic spectral features, Herit. Sci. 7 (2019). doi:10.1186/s40494-019-0249-y.

[15] P. Ricciardi, J.K. Delaney, M. Facini, J.G. Zeibel, M. Picollo, S. Lomax, M. Loew, Near infrared reflectance imaging spectroscopy to map paint binders in situ on illuminated manuscripts, Angew. Chemie - Int. Ed. 51 (2012) 5607–5610. doi:10.1002/anie.201200840.

[16] P. Ricciardi, J.K. Delaney, M. Facini, L. Glinsman, Use of imaging spectroscopy and in situ analytical methods for the characterization of the materials and techniques of 15th century illuminated manuscripts, J. Am. Inst. Conserv. 52 (2013) 13–29. doi:10.1179/0197136012Z.0000000004.

[17] M.G. Campana, M.A. Bower, M.J. Bailey, F. Stock, T.C. O'Connell, C.J. Edwards, C. Checkley-Scott, B. Knight, M. Spencer, C.J. Howe, A flock of sheep, goats and cattle: Ancient DNA analysis reveals complexities of historical parchment manufacture, J. Archaeol. Sci. 37 (2010) 1317–1325. doi:10.1016/j.jas.2009.12.036.

[18] I.D. van der Werf, C.D. Calvano, R. Laviano, A. Simonetti, L. Sabbatini, Multi-technique chemical characterisation of a 12–13th-century painted Crucifix, Microchem. J. 106 (2013) 87–94. doi:10.1016/J.MICROC.2012.05.011.

[19] R.J.H. Clark, Raman Microscopy: Application t o the Identification of Pigments on Medieval Manuscripts, Chem. Soc. Rev. 24 (1995) 187–196.

[20] C. Miliani, F. Rosi, B.G. Brunetti, A. Sgamellotti, In situ noninvasive study of artworks: The MOLAB multitechnique approach, Acc. Chem. Res. 43 (2010) 728–738. doi:10.1021/ar100010t.

[21] M. Bicchieri, M. Monti, G. Piantanida, F. Pinzari, A. Sodo, Non-destructive spectroscopic characterization of parchment documents, Vib. Spectrosc. 55 (2011) 267–272. doi:10.1016/j.vibspec.2010.12.006.

[22] M. Aceto, A. Agostino, G. Fenoglio, M. Gulmini, V. Bianco, E. Pellizzi, Spectrochimica Acta Part A : Molecular and Biomolecular Spectroscopy Non invasive analysis of miniature paintings : Proposal for an analytical protocol, Spectrochim. Acta Part A Mol.

519 Biomol. Spectrosc. 91 (2012) 352–359. doi:10.1016/j.saa.2012.02.021.
520 [23] P. Colomban, The on-site / remote Raman analysis with mobile instruments : a review
521 of drawbacks and success in cultural heritage studies and other associated fields, J.
522 Raman Spectrosc. 43 (2012) 1529–1535. doi:10.1002/jrs.4042.
523 [24] T. Cavaleri, A. Giovagnoli, M. Nervo, Pigments and mixtures identification by Visible
524 Reflectance Spectroscopy, Procedia Chem. 8 (2013) 45–54.
525 doi:10.1016/j.proche.2013.03.007.
526 [25] M. Aceto, A. Agostino, G. Fenoglio, A. Idone, M. Gulmini, M. Picollo, P. Ricciardi, J.K.
527 Delaney, Characterisation of colourants on illuminated manuscripts by portable fibre
528 optic UV-visible-NIR reflectance spectrophotometry, Anal. Methods. 6 (2014) 1488–
529 1500. doi:10.1039/c3ay41904e.
530 [26] G. Dupuis, M. Menu, Quantitative characterisation of pigment mixtures used in art by
531 fibre-optics diffuse-reflectance spectroscopy, Appl. Phys. A Mater. Sci. Process. 83
532 (2006) 469–474. doi:10.1007/s00339-006-3522-3.
533 [27] S. Lorusso, A. Natali, C. Matteucci, Colorimetry applied to the field of cultural heritage :
534 examples of study cases, Conserv. Sci. Cult. Herit. (2007) 187–220.
535 [28] G. Tempesta, C. Porfido, M. Bellino, A. Monno, The “ Exultet 1 ” of Bari : multi-
536 methodological approach for the study of a rare medieval parchment roll, Period. Di
537 Mineral. 87 (2018) 93–102. doi:10.2451/2018PM753.
538 [29] M.C. Caggiani, A. Cosentino, A. Mangone, Pigments Checker version 3 . 0 , a handy set
539 for conservation scientists : A free online Raman spectra database, Microchem. J. 129
540 (2016) 123–132. doi:10.1016/j.microc.2016.06.020.
541 [30] R. Larsen, N. Coluzzi, A. Cosentino, Free XRF Spectroscopy database of Pigments
542 Checker, Int. J. Conserv. Sci. 7 (2016) 659–668.
543 [31] A. Cosentino, FORS spectral database of historical pigments in different binders
544 Antonino, E-Conservation J. (2014) 54–65.
545 [32] C.D. Calvano, I.D. van der Werf, F. Palmisano, L. Sabbatini, Revealing the composition of
546 organic materials in polychrome works of art: the role of mass spectrometry-based
547 techniques, Anal. Bioanal. Chem. 408 (2016) 6957–6981. doi:10.1007/s00216-016-
548 9862-8.
549 [33] S. Dallongeville, N. Garnier, C. Rolando, C. Tokarski, Proteins in Art, Archaeology, and
550 Paleontology: From Detection to Identification, Chem. Rev. 116 (2016) 2–79.

551 doi:10.1021/acs.chemrev.5b00037.
552 [34] M.G. Giuffrida, R. Mazzoli, E. Pessione, Back to the past: deciphering cultural heritage
553 secrets by protein identification., Appl. Microbiol. Biotechnol. 102 (2018) 5445–5455.
554 doi:10.1007/s00253-018-8963-z.
555 [35] G. Leo, L. Cartechini, P. Pucci, A. Sgamellotti, G. Marino, L. Birolo, Proteomic strategies
556 for the identification of proteinaceous binders in paintings, Anal. Bioanal. Chem. 395
557 (2009) 2269–2280. doi:10.1007/s00216-009-3185-y.
558 [36] E. Barberis, S. Baiocco, E. Conte, F. Gosetti, A. Rava, G. Zilberstein, P.G. Righetti, E.
559 Marengo, M. Manfredi, Towards the non-invasive proteomic analysis of cultural
560 heritage objects, Microchem. J. 139 (2018) 450–457. doi:10.1016/j.microc.2018.03.033.
561 [37] D.P. Kirby, M. Buckley, E. Promise, S.A. Trauger, T.R. Holdcraft, Identification of
562 collagen-based materials in cultural heritage, Analyst. 138 (2013) 4849–4858.
563 doi:10.1039/c3an00925d.
564 [38] I.D. van der Werf, C.D. Calvano, G. Germinario, T.R.I. Cataldi, L. Sabbatini, Chemical
565 characterization of medieval illuminated parchment scrolls, Microchem. J. 134 (2017)
566 146–153. doi:10.1016/j.microc.2017.05.018.
567 [39] K.A. Dooley, S. Lomax, J.G. Zeibel, C. Miliani, P. Ricciardi, A. Hoenigswald, M. Loew, J.K.
568 Delaney, Mapping of egg yolk and animal skin glue paint binders in Early Renaissance
569 paintings using near infrared reflectance imaging spectroscopy, Analyst. 138 (2013)
570 4838–4848. doi:10.1039/c3an00926b.
571 [40] C.D. Calvano, E. Rigante, R.A. Picca, T.R.I. Cataldi, L. Sabbatini, An easily transferable
572 protocol for in-situ quasi-non-invasive analysis of protein binders in works of art,
573 Talanta. 215 (2020) 1–10. doi:10.1016/j.talanta.2020.120882.
574 [41] C.D. Calvano, E.C.L. Rigante, T.R.I. Cataldi, L. Sabbatini, In Situ Hydrogel Extraction with
575 Dual-Enzyme Digestion of Proteinaceous Binders: The Key for Reliable Mass
576 Spectrometry Investigations of Artworks, Anal. Chem. 92 (2020) 10257–10261.
577 doi:10.1021/acs.analchem.0c01898.
578 [42] E.C.L. Rigante, C.D. Calvano, R.A. Picca, S. Armenise, T.R.I. Cataldi, L. Sabbatini, Multi-
579 technique characterization of pictorial organic binders on XV century polychrome
580 sculptures by combining microand non-invasive sampling approaches, Appl. Sci. 11
581 (2021). doi:10.3390/app11178017.
582 [43] L. Micheli, C. Mazzuca, M. Missori, L. Teodonio, A. Mosca Conte, O. Pulci, L. Arcadipane,

S. Dominijanni, A. Palleschi, G. Palleschi, S. Iannuccelli, S. Sotgiu, Interdisciplinary approach to develop a disposable real time monitoring tool for the cleaning of graphic artworks. Application on “le Nozze di Psiche,” Microchem. J. 138 (2018) 369–378. doi:10.1016/j.microc.2018.01.022.

[44] P. Baglioni, M. Baglioni, N. Bonelli, D. Chelazzi, R. Giorgi, Smart Soft Nanomaterials for Cleaning, Elsevier Inc., 2018. doi:10.1016/B978-0-12-813910-3.00009-4.

[45] J.A.L. Domingues, N. Bonelli, R. Giorgi, E. Fratini, F. Gorel, P. Baglioni, Innovative Hydrogels Based on Semi-Interpenetrating p(HEMA)/PVP Networks for the Cleaning of Water-Sensitive Cultural Heritage Artifacts, Langmuir. 29 (2013) 2746–2755. doi:10.1021/la3048664.

[46] C. Mazzuca, G. Poggi, N. Bonelli, L. Micheli, P. Baglioni, A. Palleschi, Innovative chemical gels meet enzymes: A smart combination for cleaning paper artworks, J. Colloid Interface Sci. 502 (2017) 153–164. doi:10.1016/j.jcis.2017.04.088.

[47] F. Menges, Spectragryph - optical spectroscopy software, (2022).

[48] B. Lafuente, R.T. Downs, H. Yang, N. Stone, The power of databases: The RRUFF project, Highlights Mineral. Crystallogr. (2016) 1–29. doi:10.1515/9783110417104-003.

[49] A. Le Gac, Preliminary research on glues made of tawed leather, parchment and rabbit-skin, in: E. Jablonska, T. Kozielec (Eds.), Parchment Leather Heritage. Conserv., 2012: pp. 31–60.

[50] H. Plenderleith, The conservation of antiquities and works of art. Treatment, repair and restoration, Oxford University Press, London, 1971.

[51] S.C. Boyatzis, G. Velivasaki, E. Malea, A study of the deterioration of aged parchment marked with laboratory iron gall inks using FTIR-ATR spectroscopy and micro hot table, Herit. Sci. 4 (2016) 1–17. doi:10.1186/s40494-016-0083-4.

[52] E. Mannucci, R. Pastorelli, G. Zerbi, C.E. Bottani, A. Facchini, Recovery of ancient parchment: Characterization by vibrational spectroscopy, J. Raman Spectrosc. 31 (2000) 1089–1097. doi:10.1002/1097-4555(200012)31:12<1089::AID-JRS649>3.0.CO;2-C.

[53] A. Barth, Infrared spectroscopy of proteins, Biochim. Biophys. Acta - Bioenerg. 1767 (2007) 1073–1101. doi:10.1016/j.bbabio.2007.06.004.

[54] J.A. Goldsmith, S.D. Ross, Factors affecting the infra-red spectra of planar anions with D3h symmetry-II The intensity of v1 in some simple, basic and complex carbonates, Spectrochim. Acta. 22 (1966) 1069–1072. doi:10.1016/0371-1951(66)80196-0.

[55] M. Donoghue, P.H. Hepburn, S.D. Ross, Factors affecting the infrared spectra of planar anions with D3h, symmetry—V, Spectrochim. Acta Part A Mol. Spectrosc. 27 (1971) 1065–1072. doi:10.1016/0584-8539(71)80189-7.

[56] J.D. Rodriguez-Blanco, S. Shaw, L.G. Benning, The kinetics and mechanisms of amorphous calcium carbonate (ACC) crystallization to calcite, via vaterite., Nanoscale. 3 (2011) 265–271. doi:10.1039/c0nr00589d.

[57] R. Fuchs, History and biology of parchment, Karger Gaz. (n.d.).

[58] Y. Sheena Mary, L. Ushakamari, B. Harikumar, H. Tresa Varghese, C. Yohannan Panicker, FT-IR, FT-Raman and SERS Spectra of L-Proline, J. Iran. Chem. Soc. 6 (2009) 138–144.

[59] C. Sendrea, C. Carsote, E. Badea, A. Adams, M. Niculescu, H. Iovu, NON-INVASIVE CHARACTERISATION OF COLLAGEN- BASED MATERIALS BY NMR-MOUSE AND ATR-FTIR, 78 (2016).

[60] M. Odlyha, C. Theodorakopoulos, L. Bozec, Fourier transform infra-red spectroscopy (ATR / FTIR) and scanning probe microscopy of parchment, E-Preservation Sci. 6 (2009) 138–144.

[61] F. Cappa, I. Paganoni, C. Carsote, M. Schreiner, E. Badea, Studies on the effect of dry-heat ageing on parchment deterioration by vibrational spectroscopy and micro hot table method, Polym. Degrad. Stab. 182 (2020) 109375. doi:10.1016/j.polymdegradstab.2020.109375.

[62] F. Cappa, I. Paganoni, C. Carsote, E. Badea, M. Schreiner, Studies on the effects of mixed light-thermal ageing on parchment by vibrational spectroscopy and micro hot table method, Herit. Sci. 8 (2020) 1–12. doi:10.1186/s40494-020-0353-z.

[63] L. Gonzalez, M. Wade, N. Bell, K. Thomas, T. Wess, Using Attenuated Total Reflection Fourier Transform Infrared Spectroscopy (ATR FT-IR) to study the molecular conformation of parchment artifacts in different macroscopic states, Appl. Spectrosc. 67 (2013) 158–162. doi:10.1366/12-06739.

[64] S. Bruni, S. Caglio, V. Guglielmi, G. Poldi, The joined use of n.i. spectroscopic analyses - FTIR, Raman, visible reflectance spectrometry and EDXRF - To study drawings and illuminated manuscripts, Appl. Phys. A Mater. Sci. Process. 92 (2008) 103–108. doi:10.1007/s00339-008-4454-x.

[65] S. Kuckova, I. Nemec, R. Hynek, J. Hradilova, T. Grygar, Analysis of organic colouring and binding components in colour layer of art works, Anal. Bioanal. Chem. 382 (2005) 275–

282. doi:10.1007/s00216-005-3108-5.
[66] R. Vinciguerra, A. Illiano, A. De Chiaro, A. Carpentieri, A. Lluveras-Tenorio, I. Bonaduce, G. Marino, P. Pucci, A. Amoresano, L. Birolo, Identification of proteinaceous binders in paintings: A targeted proteomic approach for cultural heritage, Microchem. J. 144 (2019) 319–328. doi:10.1016/J.MICROC.2018.09.021.
[67] R. Hynek, S. Kuckova, J. Hradilova, M. Kodicek, Matrix-assisted laser desorption/ionization time-of-flight mass spectrometry as a tool for fast identification of protein binders in color layers of paintings, Rapid Commun. Mass Spectrom. 18 (2004) 1896–1900. doi:10.1002/rcm.1570.
[68] T. Tripković, C. Charvy, S. Alves, A.C.D.S. Lolić, R.M. Baošić, S.D. Nikolić-Mandić, J.C. Tabet, Identification of protein binders in artworks by MALDI-TOF/TOF tandem mass spectrometry, Talanta. 113 (2013) 49–61. doi:10.1016/j.talanta.2013.03.071.
[69] W. Fremout, S. Kuckova, M. Crhova, J. Sanyova, S. Saverwyns, R. Hynek, M. Kodicek, P. Vandenabeele, L. Moens, Classification of protein binders in artist's paints by matrix-assisted laser desorption/ionisation time-of-flight mass spectrometry: an evaluation of principal component analysis (PCA) and soft independent modelling of class analogy (SIMCA), Rapid Commun. Mass Spectrom. 25 (2011) 1631–1640. doi:10.1002/rcm.5027.
[70] P. Cicatiello, G. Ntasi, M. Rossi, G. Marino, P. Giardina, L. Birolo, Minimally Invasive and Portable Method for the Identification of Proteins in Ancient Paintings, Anal. Chem. 90 (2018) 10128–10133. doi:10.1021/acs.analchem.8b01718.
[71] J. Romero-Pastor, N. Navas, S. Kuckova, A. Rodríguez-Navarro, C. Cardell, Collagen-based proteinaceous binder-pigment interaction study under UV ageing conditions by MALDI-TOF-MS and principal component analysis, J. Mass Spectrom. 47 (2012) 322–330. doi:10.1002/jms.2966.
[72] M. Buckley, M. Collins, J. Thomas-Oaies, J.C. Wilson, Species identification by analysis of bone collagen using matrix-assisted laser desorption/ionisation time-of-flight mass spectrometry, Rapid Commun. Mass Spectrom. 23 (2009) 3843–3854. doi:10.1002/rcm.4316.
[73] B. Dolgin, V. Bulatov, I. Schechter, A complex analytical method for parchment characterization, Rev. Anal. Chem. 28 (2009) 151–307. doi:10.1515/REVAC.2009.28.3-4.151.
[74] C.J. Kennedy, T.J. Wess, The Structure of Collagen within Parchment - A Review,

679 Restaurator. 24 (2003) 61–80. doi:10.1515/REST.2003.61.
680 [75] G. Leo, I. Bonaduce, A. Andreotti, G. Marino, P. Pucci, M.P. Colombini, L. Birolo,
681 Deamidation at asparagine and glutamine As a major modification upon
682 deterioration/aging of proteinaceous binders in mural paintings, Anal. Chem. 83 (2011)
683 2056–2064. doi:10.1021/ac1027275.
684 [76] S. Hickinbotham, S. Fiddyment, T.L. Stinson, M.J. Collins, How to get your goat:
685 Automated identification of species from MALDI-ToF spectra, Bioinformatics. 36 (2020)
686 3719–3725. doi:10.1093/bioinformatics/btaa181.
687
688

689 **Captions to figures**

690

691 **Figure 1**. *Doctoratus privilegium* parchment with labelled sampled points. P = pigment analysis,
692 G = hydrogel protocol, S = in solution digestion.

693 **Figure 2**. XRF spectrum of the parchment support obtained using a portable (P) instrument. The
694 low traces of Fe, Ni, Cu and Zn belong to instrument components.

695 **Figure 3.** μ-Raman spectra comparison of cinnabar, minium and sample Pr1.

696 **Figure 4.** XRF spectra of spots Pdec and Pau1 that confirm the presence of gold and silver on
697 decorations.

698 **Figure 5**. ATR-transmittance FTIR spectra of A and B sides of parchment sample S2.

699 **Figure 6.** MALDI-MS spectrum obtained after *in situ* chymotryptic/tryptic digestion of sample
700 Gb11.

701 **Figure 7.** Tandem MS spectra of three ions obtained after hydrogel protocol application on
702 sample Gb11: (R)GARGEP(ox)GPAGLP(ox)GPP(ox)GER(G)$^{2+}$ of collagen alpha-1(I) chain, *B.*
703 *taurus*, (A); (P)QGIP(ox)GTPGRPG(V)$^{2+}$ of collagen alpha-1(XVII) chain, *B. taurus*, (B);
704 (D)AN(deam)DN(deam)FFVSG(P)$^{+}$ of collagen alpha-1(XV) chain, *O. cuniculus* (C).

705 **Figure 8**. Tandem MS spectra of a double-charged ion at *m/z* 722.3 obtained after hydrogel
706 protocol application on sample Gb11: (R)GAAGPP(ox)GATGFP(ox)GAAGR(V)$^{2+}$ of collagen alpha-
707 1(I) chain, *M. musculus* (mouse).

708 **Figure 9**. MALDI-MS spectrum of a parchment fragment, sample S1, digested in solution with
709 trypsin (A) and MS/MS fragmentation of triple-charged ion at *m/z* 961.8 corresponding to the
710 sequence (R)GLTGPIGPPGPAGAPGDKGETGP(ox)SGP(ox)AGPTGAR(G) collagen alpha-1(I), sheep
711 (B).

712

713

714

715 **Table 1.** List of the peptides retrieved in sampled points investigated by hydrogel in situ digestion.
716 Experimental and theoretical *m/z* are reported as well as relative protein as monoprotonated ion.
717 Taxonomy is considered *Bos taurus* where not differently specified.
718

Exp m/z	Theo m/z	Sequence	Protein	Gbolo2	Gb5	Gg4	Gb11	Gdec	Gr6
841.48	841.46	(R)GLPGERGR(V)	Collagen alpha-2(I)	x	x	x	x	x	x
	841.46	(R)GLPGERGR(T)	Collagen alpha-1(II)						
	841.44	(K)GEPGAPGLK(G) + 1 ox	Collagen alpha-1(III)						
868.46	868.46	(R)GPSGPQGIR(G)	Collagen alpha-2(I)	x	x	x	x	x	x
	868.43	(R)GPPGPQGAR(G) + 2 ox	Collagen alpha-1(II)						
972.45	972.39	(D)ANDNFFVSG(P) + 2 deam	Collagen alpha-1(XV) *O. cuniculus*			x	x	x	x
1052.47	1052.55	(P)QGIPGTPGRPG(V) + 1 ox	Collagen alpha-1(XVII)	x	x	x	x		x
1086.56	1086.56	(P)PGFPGAVGAKGE(G)	Collagen alpha-1(I)	x			x	x	
	1086.54	(P)SGDRGPRGER(G)	Collagen alpha-2(I)						
1105.51	1105.57	(R)GVQGPPGPAGPR(G) + 1 ox	Collagen alpha-1(I)	x	x	x	x	x	x
1110.54	1110.58	(R)GGVLFAITDAF(Q)	Collagen alpha-1(XV) *O. cuniculus*			x	x	x	x
1128.50	1128.55	(R)GLPGTPGTDGPK(G) + 2 ox	Collagen alpha-1(II)	x	x	x	x	x	x
	1128.55	(R)GLAGPPGMPGAR(G) + 3 ox	Collagen alpha-1(III)						
1144.46	1144.55	(R)GLPGTPGTDGPK(G) + 3 ox	Collagen alpha-1(II)	x	x	x	x		x
	1144.54	(R)GLAGPPGMPGAR(G) + 4 ox	Collagen alpha-1(III)						
1215.74	1215.67	(M)DQQTGNLKKAL(L)	Collagen alpha-1(I)				x		
	1215.67	(E)TLLTPEGSRKN(P)	Collagen alpha-2(I)						
1221.58	1221.63	(F)EKIEDNLITF(V)	Collagen alpha-1(XII) *O. cuniculus*	x	x		x	x	x
	1221.65	(R)EGAKGELGPPGPL(G)	Collagen alpha-3(V) *O. cuniculus*						
1241.58	1241.60	(R)GSPGGPGAAGFPGGR(G)	Collagen alpha-1(III)	x	x	x	x	x	x
1267.59	1267.68	(R)GIPGPVGAAGATGAR(G) + 1 ox	Collagen alpha-2(I)		x	x	x	x	x
1289.50	1289.59	(R)GSPGGPGAAGFPGGR(G) + 3 ox	Collagen alpha-1(III)			x	x		
1427.53	1427.70	(R)GSAGPPGATGFPGAAGR(V)	Collagen alpha-1(I)	x	x	x	x	x	x
	1427.73	(R)GIPGEFGLPGPAGAR(G) + 2 ox	Collagen alpha-2(I)						
	1427.79	(K)ALLIQGSNDVEIR(A)	Collagen alpha-1(II)						
1435.49	1435.68	(R)GEPGPAGLPGPPGER(G) + 3 ox	Collagen alpha-1(I)	x	x	x	x	x	x
	1435.69	(R)GPPGPPGTNGVPGQR(G) + 3 ox	Collagen alpha-1(III)						
1443.57	1443.70	(R)GAAGPPGATGFPGAAGR(V) + 2 ox	Collagen alpha-1(I) *M. musculus*	x			x	x	
1459.50	1459.69	(R)GSAGPPGATGFPGAAGR(V) + 2 ox	Collagen alpha-1(I)	x	x	x	x	x	x
1473.48	1473.67	(R)GDGGPPGATGFPGAAGR(T) + 2 ox	Collagen alpha-2(I)		x	x		x	x
1550.73	1550.81	(K)EGLRGPRGDQGPVGR(S)	Collagen alpha-2(I)	x			x		
1560.77	1560.73	(K)STGISVPGPMGPSGPR(G) + 4 ox	Collagen alpha-1(I)		x	x	x		
1562.60	1562.79	(R)GDKGETGEQGDRGIK(G) + 1 ox	Collagen alpha-1(I)		x	x	x		
	1562.83	(K)GAAGLPGVAGAPGLPGPR(G) + 3 ox	Collagen alpha-2(I)						
1568.74	1568.73	(K)NSVAYMDQQTGNLK(K)	Collagen alpha-1(I)				x		
1586.72	1586.74	(K)GNSGEPGAPGSKGDTGAK(G)	Collagen alpha-1(I)		x	x	x	x	x
	1586.70	(R)GETGPAGPSGAPGPAGSR(G) + 4 ox	Collagen alpha-1(III)						
1648.76	1648.78	(K)AGEDGHPGKPGRPGER(G) + 2 ox	Collagen alpha-2(I)			x	x		
1693.66	1693.78	(R)GYPGSIGPTGAAGAPGPHGSVGPAG K(H) + 3 ox	Collagen alpha-1 (V) *M. musculus*	x	x	x	x		x

1709.79	1709.75	(K)GENGVPGEDGAPGPMGPR(G) + 1 ox	Collagen alpha-1(III) *O. cuniculus*		x	x	x		
1719.77	1719.84	(R)GARGEPGPAGLPGPPGER(G) + 3 ox	Collagen alpha-1(I)	x	x	x	x		
1832.81	1832.81	(R)GPPGPMGPPGLAGPPGESGR(E) + 3 ox	Collagen alpha-1(I)		x	x	x		
1868.84	1868.91	(R)GERGEAGSPGIAGPKGEDGK(D)	Collagen alpha-1(III)	x			x		
1921.86	1921.91	(R)GQEITVRGSETSHCFTGL(S)	Collagen alpha-1(XII) *O. cuniculus*	x	x	x	x	x	x
	1921.91	(K)SGDRGETGPAGPSGAPGPAGAR(G)	Collagen alpha-1(III) *O. cuniculus*						
1922.86	1922.93	(R)GERGPPGESGAAGPTGPIGSR(G) + 1 ox	Collagen alpha-2(I)	x	x	x	x	x	x
	1922.86	(K)GDSGAPGERGPPGAGGPPGPR(G) + 5 ox	Collagen alpha-1(III)						
1975.90	1975.99	(K)SGDRGETGPAGPAGPIGPVGAR(G)	Collagen alpha-1(I)	x	x	x	x		x
	1975.95	(K)GEPGAVGQPGPPGPSGEEGKR(G)	Collagen alpha-2(I)						
	1976.03	+ 1 ox (R)GPPGPQGARGFPGTPGLPGVK(G) + 2 ox	Collagen alpha-1(II)						
2028.08	2028.08	(K)TGVPSFTKPVPPTQKPAPF(T) + 2 ox	Collagen alpha-I(XXVII) *M. musculus*				x	x	
2092.92	2093.00	(R)EGREGEKGSKGEPGPDGPPGR(T)	Collagen alpha-3(V) *O. cuniculus*	x			x		
2130.99	2131.03	(R)GVQGPPGPAGPRGANGAPGNDGAK (G) + 2 ox	Collagen alpha-1(I)	x	x	x	x	x	x
	2131.11	(R)GLPGVAGSVGEPGPLGIAGPPGAR(G) + 3 ox	Collagen alpha-2(I)						
	2130.95	(R)GMPGPQGPRGDKGETGEAGER(G) + 3 ox	Collagen alpha-1(II)						
2265.09	2265.09	(R)GYPGSIGPTGAAGAPGPHGSVGPAG K(H) + 3 ox	Collagen alpha-2(I) *M. musculus*		x		x		x

719

720

721

722 **Table 2.** Proteomics data of the parchment sampled points (*Doctoratus privilegium*) obtained by
723 MALDI-ToF-MS and RPLC-ESI(+)-MS/MS using two types of sample digestions.

Sample*	*In situ* trypsin & chymotrypsin digestion	In-solution trypsin digestion	Sample description
Gb5	✓	-	Bovine and rabbit glue painting binder Mouse collagen residues
Gb11	✓	-	Bovine and rabbit glue painting binder Mouse collagen residues
Gbolo2	✓	-	Bovine and rabbit glue painting binder Mouse collagen residues
Gdec	✓	-	Bovine and rabbit glue painting binder Mouse collagen residues
Gg4	✓	-	Bovine and rabbit glue painting binder Mouse collagen residues
Gr6	✓	-	Bovine and rabbit glue painting binder Mouse collagen residues
S1	-	✓	Sheep skin parchment
S2	-	✓	Sheep skin parchment
S3	-	✓	Sheep skin parchment

724 * Labelled sample zones are depicted in Figure 1.

725

726

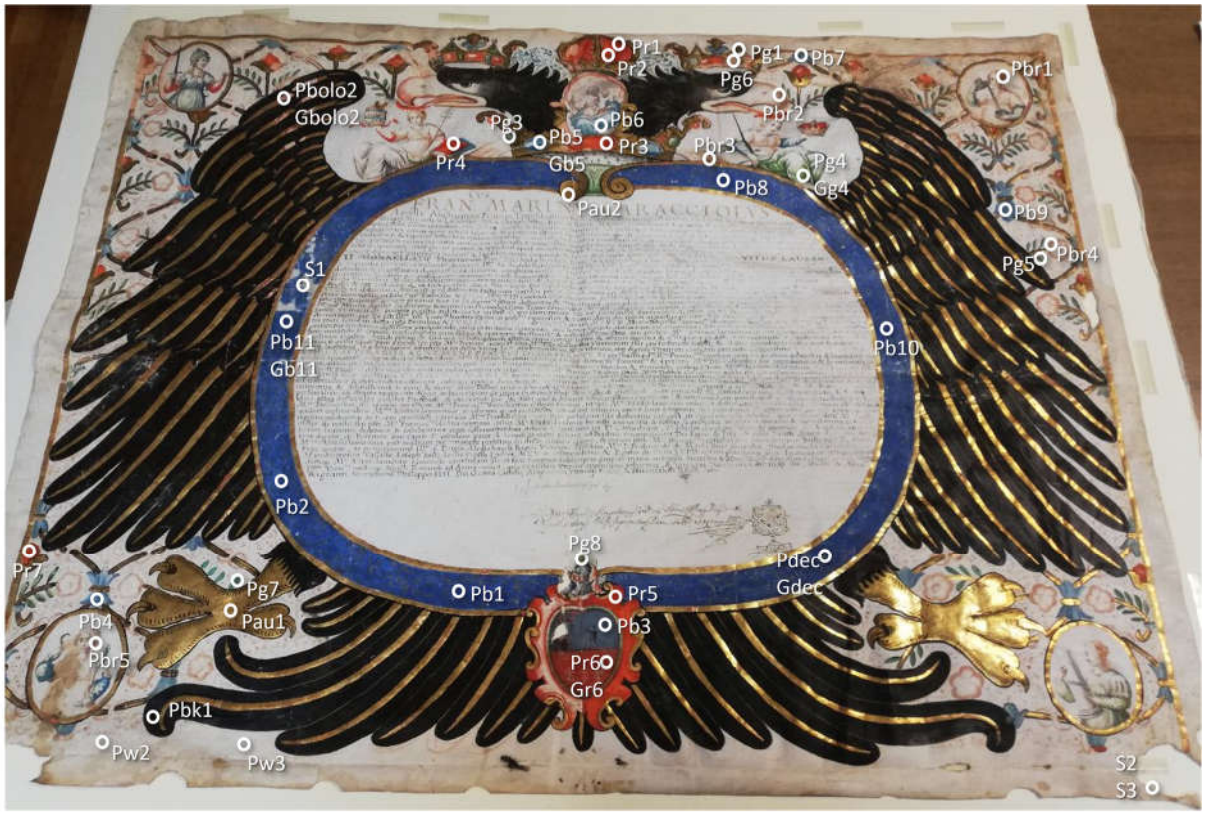

Figure 1.

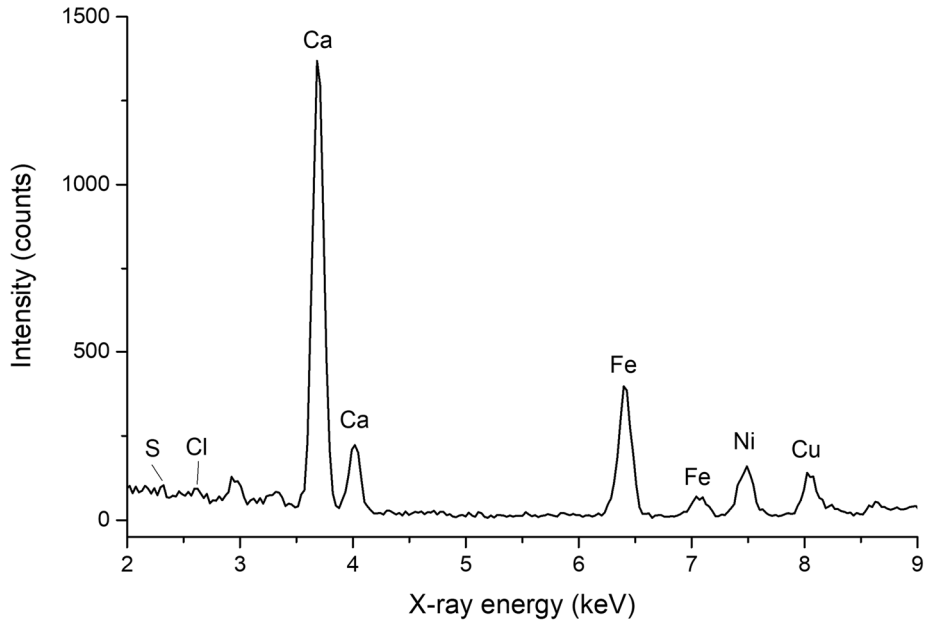

Figure 2.

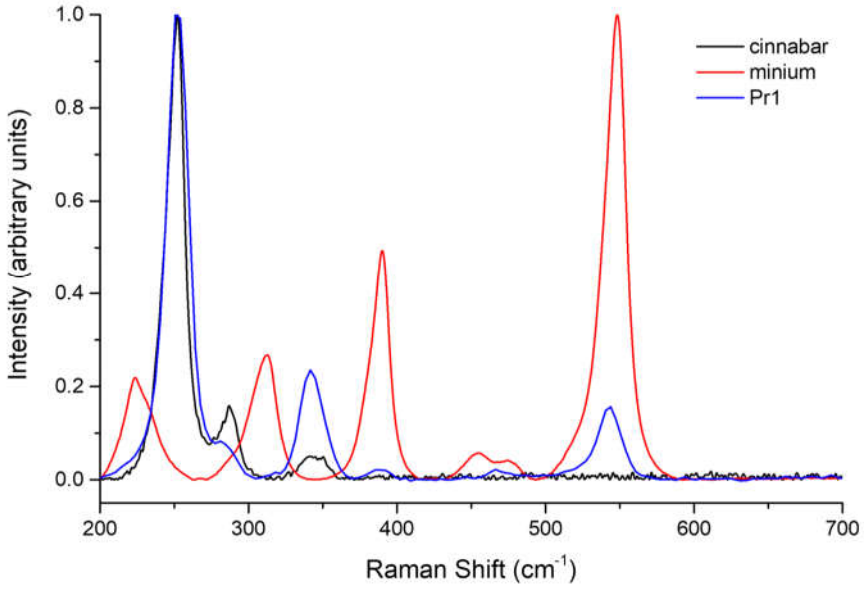

Figure 3.

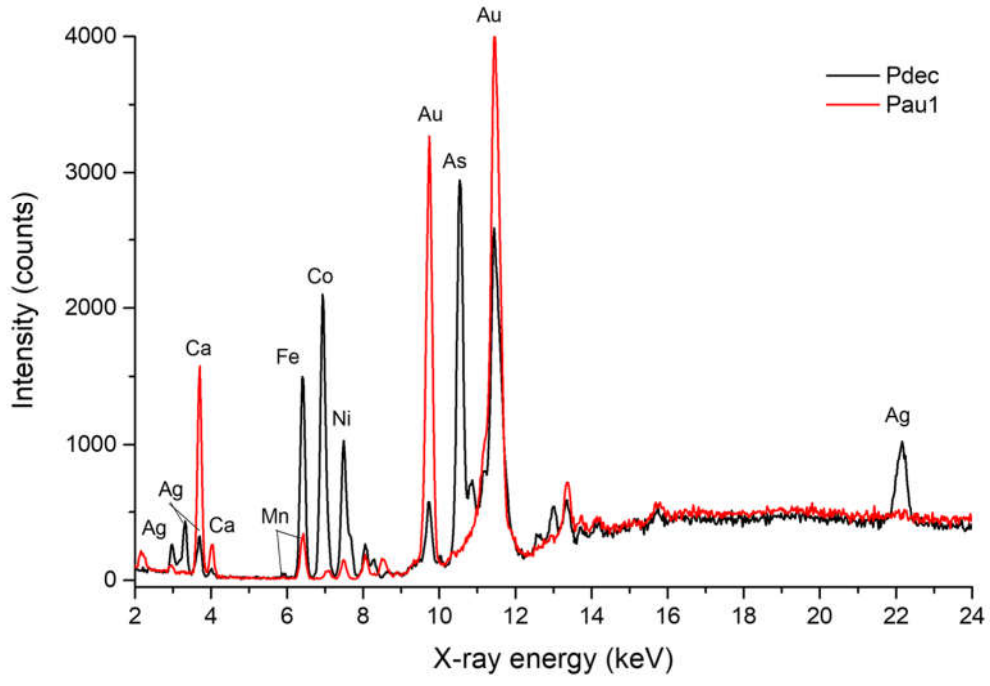

Figure 4

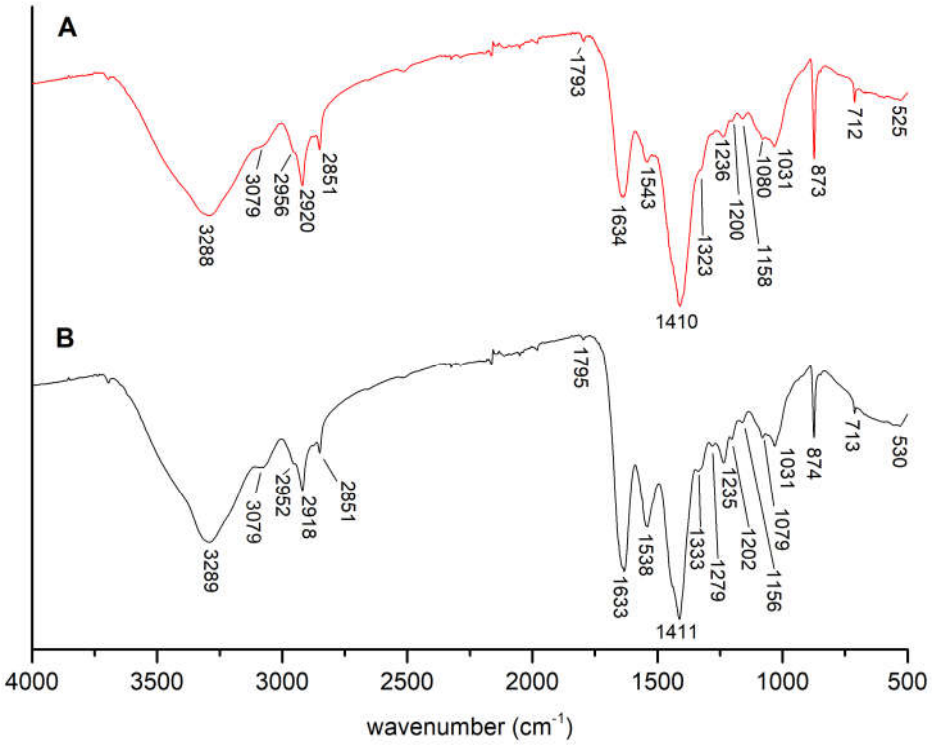

746

747 **Figure 5**

748

749

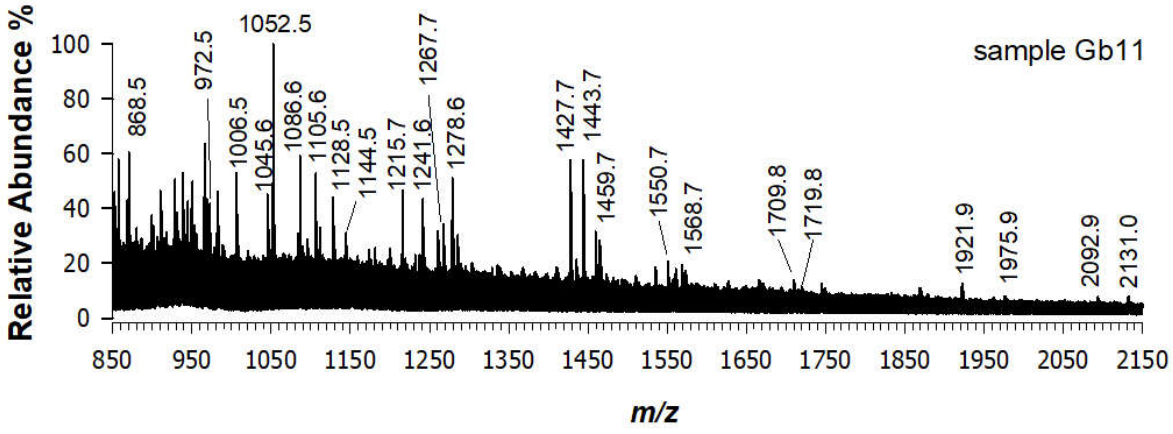

750

751 **Figure 6**

752

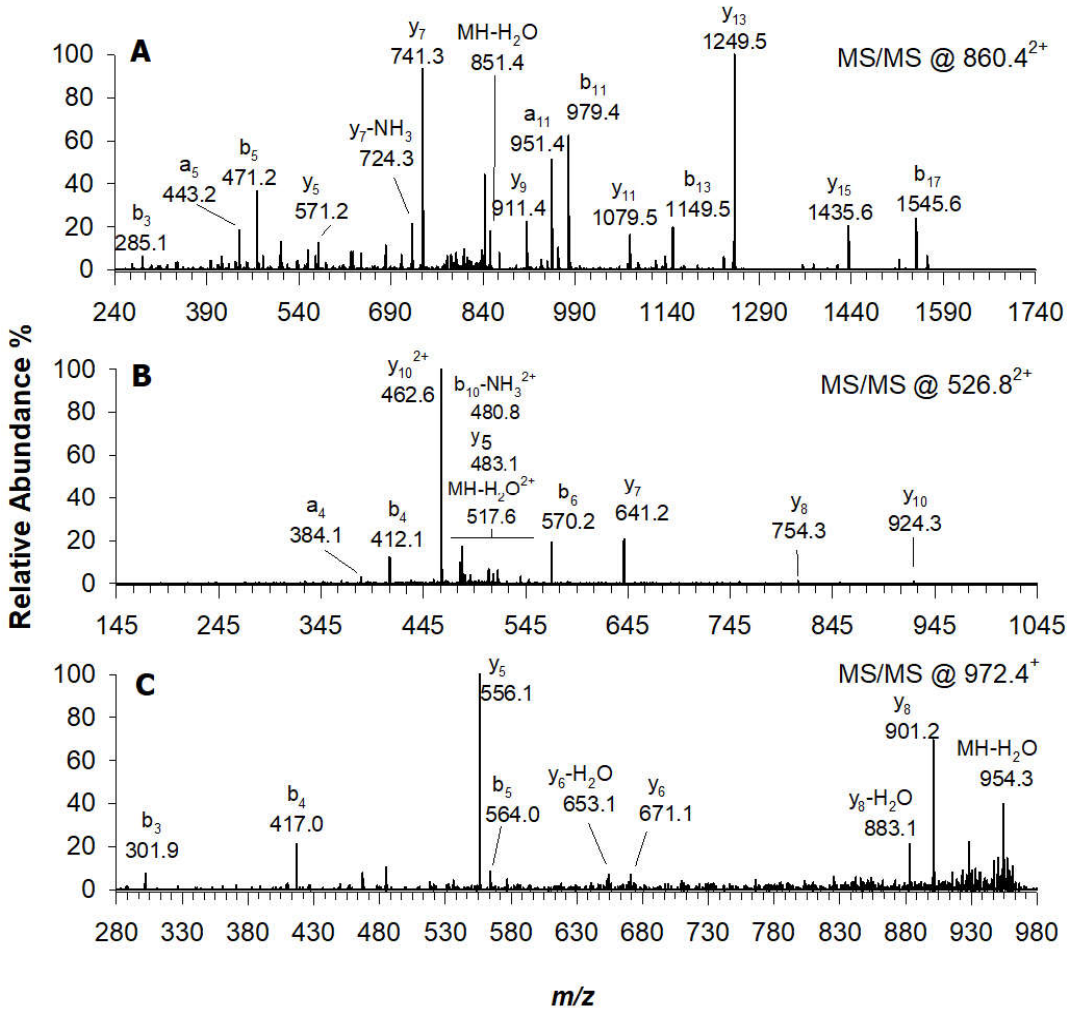

753

754 **Figure 7**

755

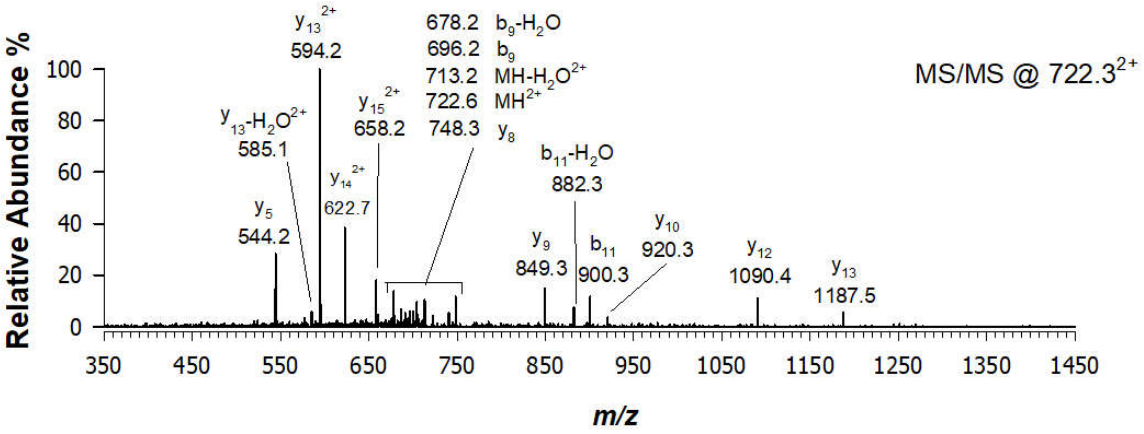

756

757 **Figure 8**

758

759

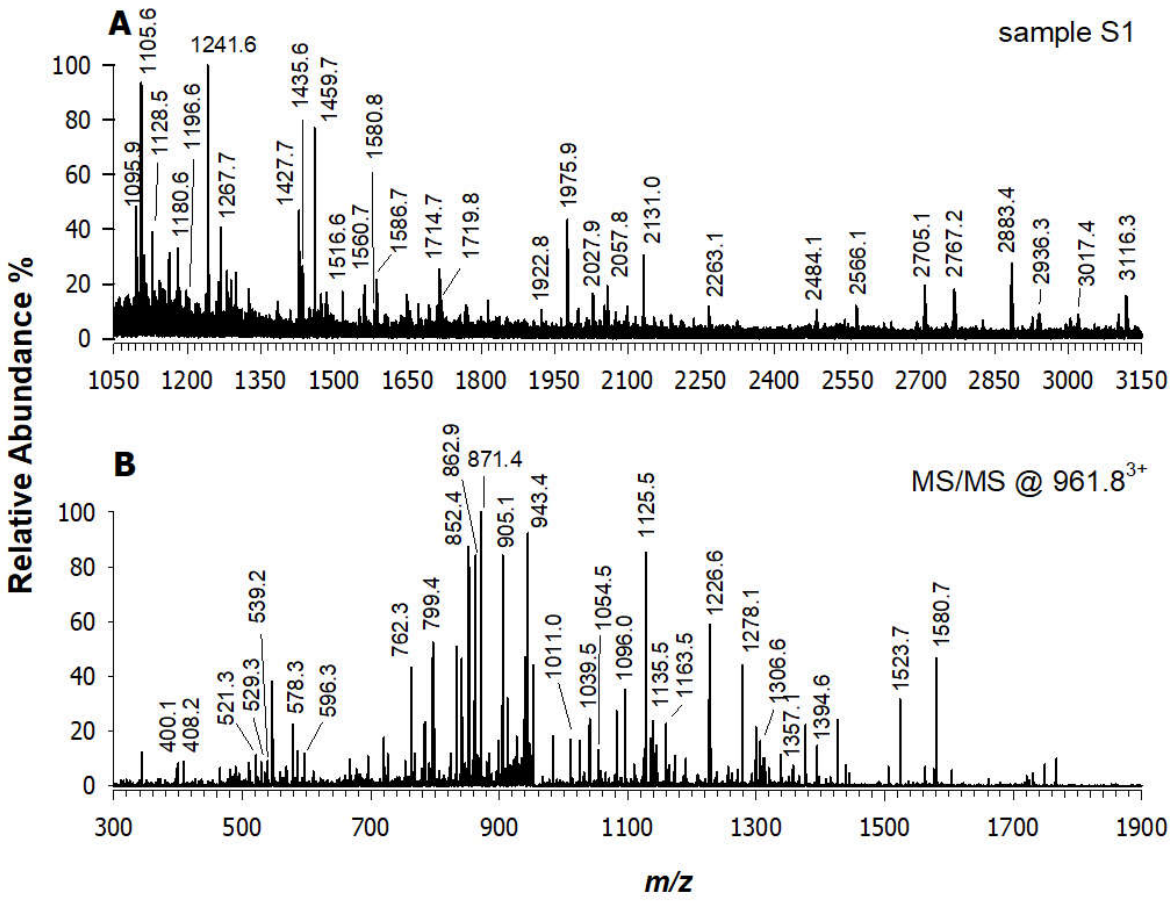

760

761 **Figure 9**